Classical-trajectory Monte Carlo calculations of the electronic stopping cross section for keV protons and antiprotons impinging on hydrogen atoms

Ernesto R. Custidiano* and Mario M. Jakas†
Departamento de Física Fundamental y Experimental, Electrónica y Sistemas, Universidad de La Laguna, 38205 La Laguna, Tenerife, Spain
(Received 11 February 2005; published 15 August 2005)

Using the classical-trajectory Monte Carlo (CTMC) method, the electronic stopping cross sections of hydrogen atoms by protons and antiprotons impact are calculated. The results show that the CTMC method compares fairly well with previous quantum mechanics calculations of the stopping cross sections for the same colliding pairs. It turns out therefore that the CTMC method constitutes a reliable and, computationally speaking, convenient alternative to calculate the stopping of ions in matter. The present results also show that the stopping appears to be particularly sensitive to the angular momentum (L) of the electron orbit. In the case of protons, the highest sensitivity to L becomes evident around the energy of the maximum stopping. While for antiprotons the largest sensitivity of the stopping to L is observed down at low bombarding energies, i.e., below 10 keV.

DOI: 10.1103/PhysRevA.72.022708 PACS number(s): 34.10.+x, 34.50.Bw, 87.64.Aa

I. INTRODUCTION

Although classical mechanics is not expected to accurately describe the response of the electronic system during the scattering of atomic species, classical models frequently appear in the atomic collision literature [1–5] (and references therein). In the case of stopping the situation appears to be even more striking, since a model as simple as the classical harmonic oscillator (CHO) has been recurrently utilized since it was first introduced by Bohr in 1913 [6] and used to calculate the stopping cross section,

$$S_B = \frac{e^4}{4\pi\,\epsilon_0^2 m\,v^2}\ln\left(\frac{14.112\,\epsilon_0 m\,v^3}{\omega\,e^2}\right), \tag{1}$$

where e is the elementary charge, m is the electron mass, v is the projectile velocity, ϵ_0 is the vacuum permittivity, and ω is the frequency of the harmonic oscillator.

The success of the CHO seems to be, however, well justified, because this model is observed to account for the stopping of high-energy ions in matter to within a remarkable degree of accuracy and, as recent calculations showed [7], it also seems to work fairly well down at low energies.

Admittedly, the advantage of a classical over a quantum approach is clear. This stems from the fact that the motion of a classical particle can be readily solved, whereas on the quantum side, not only are more elaborate numerical techniques required, but also several approximations have to be introduced to calculate the time evolution of the electron wave function. See, for example, the Bethe-Born expression

$$S_{BB} = \frac{e^4}{4\pi\,\epsilon_0^2 m\,v^2} Z_T\left[\ln\left(\frac{2m\,v^2}{\bar{I}}\right) - 1 - \frac{C}{Z_T}\right], \tag{2}$$

where Z_T is the atomic number of the target atom, $\bar{I}$ is the mean ionization potential of the target electrons, and C is a numerical constant associated with the shell structure of the target atom. This equation was obtained by Bethe and Jackiw [8] using the first-order Born approximation. Therefore it may be accurate at large ions velocities but fails when the ion velocity becomes similar to or lower than that of the more external electrons in the target atom. On the low velocity regime the situation is not better either. Apart from early papers [9–11] which produced estimates of the stopping cross section from simple arguments, recent calculations, though more elaborate, are based on the assumption that the target electrons are part of a homogeneous Fermi condensate, i.e., the electron gas [12–14]. Thus these models may be appropriate for solid materials but one cannot expect them to be accurate enough in the case of atomic targets.

Curiously enough, it was not until recently that the stopping was calculated by solving the Schrödinger equation [15,16] in such a way that one can regard them as the quantum equivalent of the classical simulations. To this end, Schiwietz [15] projected the electron state into a complete base of atomic orbitals and, then, solved the Schrödinger equation using the so-called time-dependent close-coupling method, whereas Trujillo *et al.* used a computational quantum-mechanics approach known as the time-dependent variational principle (see Ref. [17] and references therein).

Going back to classical calculations, one finds that no attempt at going beyond the CHO model and calculating the stopping cross section using a potential other than the harmonic has been reported. Therefore as yet it is not clear whether the apparent success of classical calculations of the stopping is nothing other than the result of a fortuitous cancellation of errors, i.e., those introduced by the use of clas-

*Permanent address: Departamento de Física, Facultad de Ciencias Exactas y Naturales, y Agrimensura, Universidad Nacional del Nordeste, Avda, Libertad 5600, 3400 Corrientes, Argentina. Electronic address: cernesto@exa.unne.edu.ar
†Electronic address: mmateo@ull.es

sical mechanics on the one hand and the harmonic potential on the other.

In order to investigate along such a direction, this paper presents a comparison of the results of calculating the stopping cross section of hydrogen atoms by collision with protons and antiprotons using the CTMC method, and those of previous quantum calculations for the same colliding pairs in Refs. [15]and [16]. According to the present calculations, the classical approximation appears to reproduce available quantum calculations fairly well. Moreover, the difference predicted by quantum calculations for protons and antiprotons are nicely reproduced by the classical model. It turns out therefore that the so-called classical-trajectory Monte Carlo method [1] seems to be a quite reliable technique for calculating the stopping cross section of a hydrogen atom by proton and antiproton impact.

II. CTMC CALCULATIONS

Calculations in this paper are based on a computer simulation technique known as classical trajectory Monte Carlo (CTMC). It works by numerically solving the motion of the classical electron in the target atom during the passage of the bombarding ion (see Ref. [18]). By repeating such an event or *history* a number of times, the stopping cross section can be readily obtained. Such a number is normally the result of a compromise between the running time and the requested statistical error. In this paper, one thousand to one hundred thousand histories are normally required to reach uncertainties of the order of 10%, or smaller. Depending on the case, execution times may take between a few minutes up to a couple of hours running on a 1.2-GHz Pentium based PC. As is often the case in the CTMC method, one history differs from the other by the initial position and velocity of the electron in the target atom. In this paper, the initial velocity and position of the electron are picked at random following the procedure that is described in Ref. [19]. Accordingly, electrons are prepared in such a way that they are found initially moving on randomly oriented orbits with a binding energy $U_0=-13.6$ eV, and an eccentricity ε picked at random assuming that ε^2 is a random, uniformly distributed variable.

It must be mentioned that no energy transfer between the nuclei is assumed in the present calculations. Actually, the possibility of exchanging energy between the projectile and target nuclei is included in this CTMC code, but it turned out to be negligibly small even at the lowest bombarding energy studied in this paper. As a matter of fact, except for small impact parameters, the Coulomb repulsion (attraction) between the incoming proton (antiproton) and the target nucleus is observed to produce negligible deflections. Therefore as far as the stopping is concerned and within the bombarding energy range in this paper, one can readily conclude that the so-called *straight-line approximation* works remarkably well.

III. RESULTS AND DISCUSSION

The stopping cross sections for protons impinging on hydrogen are plotted in Fig. 1. It shows experimental data from Refs. [20–24], theoretical results using quantum mechanics from Schiwietz [15] and Cabrera-Trujillo *et al.* [16], and the present CTMC calculations. As one can readily see, the CTMC results compares fairly well to both experimental data and quantum results. This is particularly so at energies larger than E_{max}, i.e., the energy at which the stopping cross section reaches its maximum value (S_{max}). As a matter of fact, in this high-energy regime quantum calculations and CTMC results compare to experimental data remarkably well. At energies smaller than E_{max} theoretical results deviate from the experiments. However, this is not at all unexpected, since at low ion velocities protons turn into neutral hydrogen after a few collisions and therefore the contribution of neutral hydrogen to the total stopping has to be included. This is something, however, which is not included in the present CTMC results or in the quantum calculations that appear in Fig. 1. In addition to this, it must be taken into account that the experiments use H_2 as a target, and not atomic hydrogen as assumed in the calculations. This may also account for the observed discrepancy, but, unfortunately, the present CTMC code is not prepared to deal with both neutral projectiles or a molecular target.

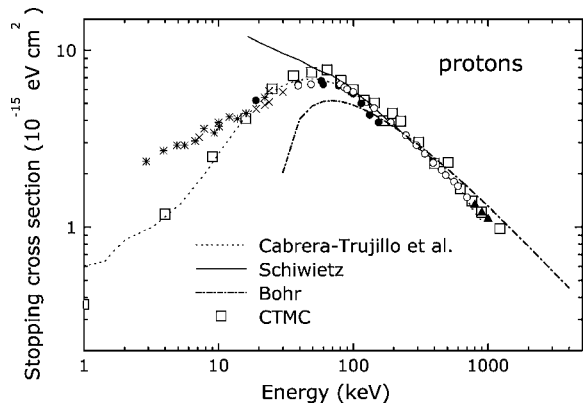

FIG. 1. Stopping cross section for protons impinging on hydrogen. Symbols show the experimental data from Refs. [20] (×), [21] (○), [22] (•), [23] (▲), and [24] (*). Lines are quantum-mechanics calculations after Schiwietz [15] (continuous) and Cabrera *et al.* [16] (dotted). The classical Bohr predictions [6] are plotted as a dashed line. Open squares indicate the results of the present CTMC calculations.

It should be noted that below the energy of the maximum stopping the theoretical results in Ref. [15] become fairly large. The origin of such a discrepancy can be attributed to the fact that calculations in Ref. [15] are based on an expansion of the electron wave function in terms of the eigenfunctions of the target atom. Since at low bombarding energies the stopping proceeds mainly from collisions where the electron is captured by the incoming ion (see below), it is clear that using atomic orbitals centered on the target cannot adequately describe an electron that moves away with the ion. Thus it is to some extent to be expected that the results in Ref. [15] fail at low bombarding energies. Interestingly enough, the present CTMC calculations show an excellent agreement with those in Ref. [16] a result that must be emphasized, since calculations in Ref. [16] were obtained using a numerical technique that is assumed to be an accurate

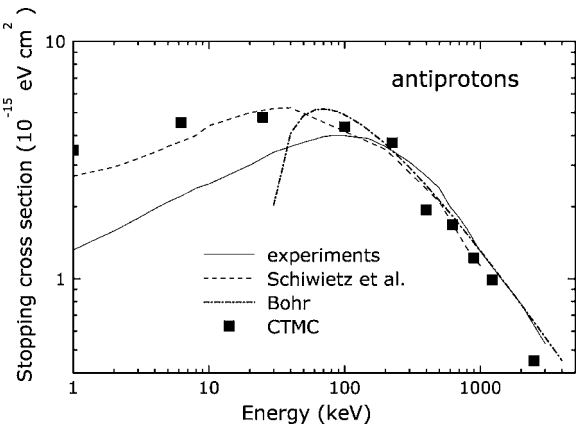

FIG. 2. Stopping cross section for antiprotons ($\bar{p}$) impinging on hydrogen. The continuous line shows experimental data for $\bar{p}$ on H_2 in Ref. [25]. The dotted line denotes the theoretical results for $\bar{p}$ on H from Ref. [26] and the dashed line shows the classical results of Bohr [6]. Full squares show the present CTMC calculations.

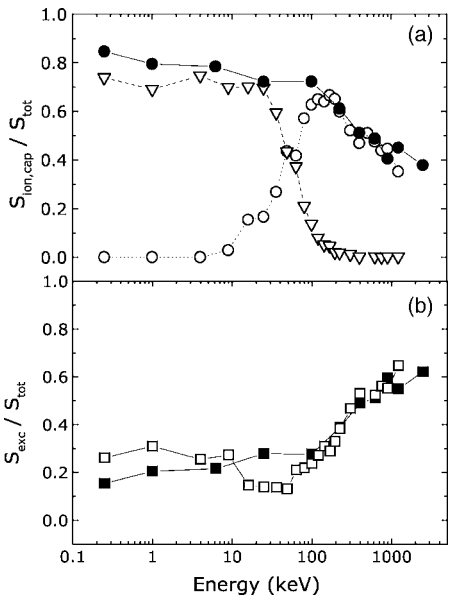

FIG. 3. Fraction of the stopping for collisions that resulted in either ionization (S_{ion}/S_{tot}), excitation (S_{exc}/S_{tot}) of the target, or capture (S_{cap}/S_{tot}) of the target electron by the projectile. Open symbols stand for protons that produced ionization (○), capture (▽) and excitation (□), whereas full symbols denote the cases of ionization (●) and excitation (■) by antiprotons.

method of solving the time-dependent Schrödinger equation (see Ref. [17]).

The stopping cross sections for antiprotons ($\bar{p}$) impinging on H and H_2 targets are plotted in Fig. 2. The agreement between experimental data and theoretical results appears to be fairly good. Admittedly though, at low bombarding energies deviations between experiments and theoretical calculations are clearly observed. As electron capture has to be disregarded this time, such discrepancies can be attributed to the fact that the stopping is measured on a H_2 target, whereas calculations are performed for atomic hydrogen. Of course this may not necessarily be the case but, again, the present simulations cannot be used to rule out such a hypothesis. It must be noted thoughout that the CTMC results compare remarkably well with the quantum calculations in Ref. [15].

For the sake of completeness, however, Bohr's classical predictions [6], given by Eq. (1), are also plotted in Figs. 1 and 2. The frequency of the harmonic oscillator (ω) in Bohr's model is replaced by $\omega=2\pi/T$, where T is the period of the classical electron in its orbit around the target nucleus, i.e., $T=(e^2/2m\epsilon_0)[m/(2|U_0|)]^{3/2}$, where U_0 is the binding energy of the target electron. Bohr's predictions seem to work remarkably well at large bombarding energies. This is not surprising though, since, except for small corrections, namely the *inner shell* or the Barkas effect [27], the CHO model is recognized for being a highly accurate model above the energy of the maximum stopping.

Another interesting aspect of the stopping of hydrogen by p and $\bar{p}$ collisions is illustrated in Figs. 3(a) and 3(b). There, one can see S_{ion}/S_{tot}, S_{cap}/S_{tot}, and S_{exc}/S_{tot}, denoting the fraction of the stopping cross section that is associated with trajectories that ended up producing the ionization, the capture, or the excitation of the electron by the incoming projectile. It must be noted, however, that, since capture cannot take place for antiprotons, only the ionization contributions to stopping appear in this case. As one can readily see, at low bombarding energies, capture appears to be strongly linked to the stopping of protons. Actually, below 10 keV about 70% of the stopping proceeds from collisions that have produced electron capture, whereas excitation accounts for the remaining 30% and ionization plays scarcely any role in the stopping of slow protons. With an increase of the bombarding energy the importance of capture drops and, approximately around the energy of the maximum stopping, both ionization and excitation become the two dominating processes. As a matter of fact, the contribution of ionization to stopping appears to reach a maximum at approximately 200 keV and, at larger energies, the stopping is equally shared between collisions that resulted in the ionization and the excitation of the target electron. And the latter applies to both proton and antiproton projectiles.

In the case of antiprotons, ionizing collisions amount to 80% of the stopping at 1 keV. With an increase of the energy such a fraction decreases slowly to reach 60% at 100 keV. At larger energies it starts dropping at a faster rate, becoming 32% of the total stopping at the largest bombarding energy calculated in this paper, namely 2.5 MeV. From the results in Fig. 3 one can also conclude that the fraction of energy that goes into excitation appears to be, approximately, a monotonouosly increasing function of the bombarding energy. Such a function, moreover, shows little dependence on the sign of the projectile charge.

As was mentioned in a previous paper[19], the initial distribution of the electron has noticeable effects on the CTMC calculation of the ionization and capture cross sections. In order to verify whether or not the stopping shows a similar sensitivity to the initial distribution, the procedure in Ref. [19] was slightly modified so that, instead of choosing the eccentricity at random, as in the original version of the algorithm, it may optionally draw orbits with a fixed eccentricity.

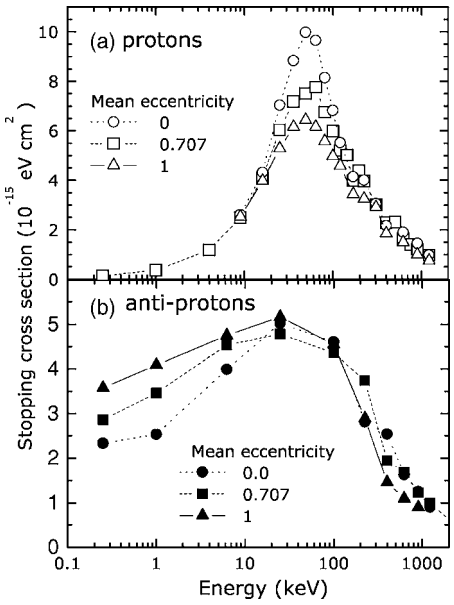

FIG. 4. Influence of the eccentricities of the orbits in the initial distribution of the target electron upon the stopping cross section for (a) protons and (b) antiprotons impinging on hydrogen atoms.

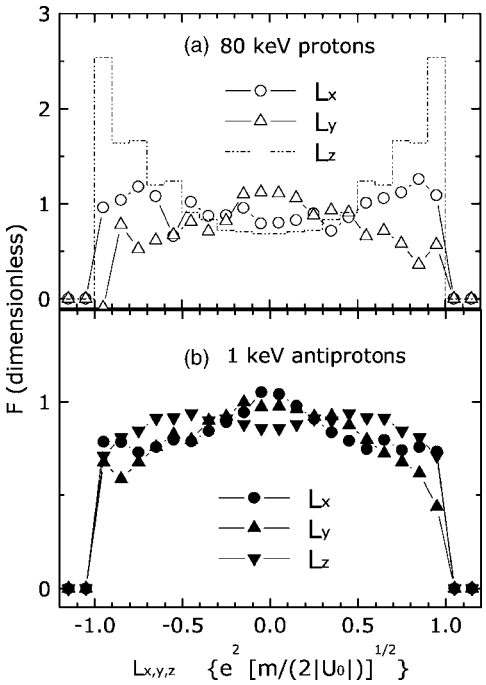

FIG. 5. Contribution to stopping from electrons initially orbiting around the target nucleus with an angular momentum (L_n, dL_n), where $n=x,y,z$ [see Eq. (3)]. These results stand for (a) 80-keV protons and (b) 1-keV antiprotons and, in both cases, initial eccentricities are obtained using the procedure in Ref. [19].

In this way, the stopping cross sections are calculated for eccentricities $\varepsilon=0$, 0.707, and 1. Here, the case denoted as $\varepsilon=0.707$ stands for the calculations using randomly distributed eccentricities, that were already plotted in Figs. 1 and 2.

The results of such calculations are displayed in Figs. 4(a) and 4(b). There, one can see that the influence of the eccentricity on the stopping is evident and in such a way that it depends on the sign of the projectile charge. In the case of protons the stopping seems to exhibit a fairly large sensitivity to ε around the energy of the maximum stopping. Actually, S_{max} is observed to be a decreasing function of ε. At energies larger than E_{max} the same dependence upon ε seems to hold, but it becomes attenuated as the energy gets larger. Below E_{max}, however, no sign of sensitivity upon the eccentricity is observed.

In the case of antiprotons the stopping shows a fairly large dependence on the eccentricity at low bombarding energies. As a matter of fact, below 10 keV there seems to be three well-separated curves, that of $\varepsilon=0$ being the lower one, and above the three of them is that of $\varepsilon=1$. At higher energies, however, the results for the three eccentricities, i.e., $\varepsilon=0$, 0.707, and 1 grouped into a single curve, thus showing that eccentricity plays almost no role in the stopping for antiprotons bombarded with energies greater than, say, 30 keV.

It must be noted that for both protons and antiprotons E_{max} does not appear to be a function of ε. Such a result can be ascribed to the fact that the maximum of the stopping is expected to occur when the projectile velocity becomes similar to that of the electron in the target atom and, according to the procedure used in this paper, the mean-squared value of the initial electron velocity depends on the binding energy, but not on ε.

Since the eccentricity is connected to angular momentum (L), i.e., $L=e^2[m(1-\varepsilon^2)/(2|U_0|)]^{1/2}$, the results above show that the stopping cross section is sensitive to L as well. Remarkably though, a similar effect was already observed in Ref. [28], where CTMC calculations of the charge-exchange, ionization, and excitation cross sections showed a substantial dependence on the initial angular momentum of the electron. In the case of stopping, one can go further and analyze the result of calculating $F(L_n)$, namely the contribution to the stopping from electrons that have had an initial angular momentum within the range (L_n, dL_n) for $n=x,y,z$. This function can be more formally defined as

$$F(L_n) = \frac{1}{P(L_n)S}\frac{dS}{dL_n}, \tag{3}$$

where S is the total stopping cross section, and $P(L_n)$ is the probability distribution of the initial angular momentum L_n.

The results of calculating $F(L_n)$ for 80-keV protons and 1-keV antiprotons are displayed in Figs. 5(a) and 5(b). These two cases were chosen because these are, approximately, the energies at which the stopping of protons and antiprotons exhibited the largest sensitivity to eccentricity. As is expected for a classical electron, the angular momentum cannot be larger than $L_{max}=e^2[m/(2|U_0|)]^{1/2}$, therefore no data can appear beyond such a value. It is worth noting that the dependence of F upon the initial distribution of ε is partially removed after dividing the results by $P(L_n)$ [see Eq. (3)]. However, the removal is not complete and the results plotted in Figs. 5(a) and 5(b) may still depend on the initial distribution of ε, namely that in Ref. [19].

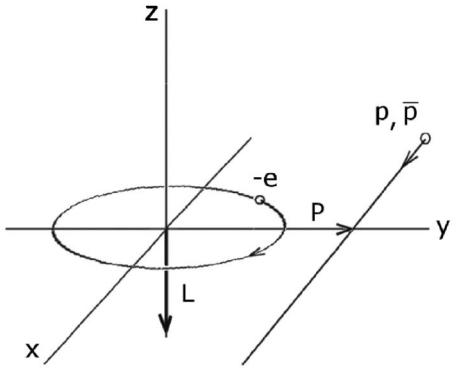

FIG. 6. Electron moving on orbit with a small eccentricity and a large, negative L_z.

In the case of protons, one can readily see that large values of L_z, in an absolute sense, are clearly linked to large stopping cross sections, whereas small angular momenta show no correlation to large stopping. In order to understand these results one must bear in mind that in the simulations the projectile moves along the x direction and the impact parameter is on the y axis. Therefore as a large $|L_z|$ is associated with electrons which are orbiting on the same plane as that of the proton scattering and, when close to the projectile, these electrons may possibly have a small relative velocity with respect to the incoming projectile (see Fig. 6), it is thus obvious that these orbits are more amenable to absorbing energy from the bombarding ion than any other.

The results look quite different for 1-keV antiprotons. In this case, the angular momentum appears to be anticorrelated to the stopping cross section. Therefore electrons with a large angular momentum, in an absolute sense, are expected to produce smaller stopping cross sections compared to those with a small L. The origin of this behavior is not wholly clear to the present authors. However, it seems to be connected to the fact that low-energy antiprotons push the electron away from the target nucleus, thus promoting the electron to a high-energy orbit and, as a result, the electron may become either excited or ionized. According to this picture, it is obvious that large-L electrons are more amenable to being excited or ionized compared with those with small L, because the former are moving, all the time, at a large distance from the nucleus, whereas in small-L orbits the electron must approach the nucleus at every turn and at least, then, the electron may not be as susceptible to being displaced from its trajectory as might be in the case of a large-L orbit. It must be noted though that a small enhancement of the stopping for large $|L_z|$ is observed, but it does not seem to be as large as in the case of 80-keV protons.

IV. CONCLUSIONS

Classical-trajectory Monte Carlo (CTMC) calculations of the stopping cross section of hydrogen by proton and antiproton collisions are presented. The results appear to agree with experiments and previous theoretical calculations fairly well. It turns out therefore that the CTMC method constitutes a reliable means to calculate the stopping of hydrogen atoms by proton and antiproton impact over a wide range of bombarding energies. The present results also suggest that the stopping cross section is sensitive to the eccentricity—or the angular momentum—of the electron orbit. Such a sensitivity becomes particularly high at a range of the bombarding energy which depends on the sign of the projectile charge. For protons the influence of eccentricity becomes apparent around the maximum of the stopping, whereas for antiprotons the largest sensitivity is observed at low bombarding energy, i.e., below the energy of the maximum stopping.

ACKNOWLEDGMENT

The authors acknowledge with thanks the financial support received from the Universidad de La Laguna through the Oficina de Relaciones Internacionales.

[1] R. E. Olson and A. Salop, Phys. Rev. A **16**, 531 (1977).
[2] R. L. Becker and A. D. MacKellar, J. Phys. B **12**, L345 (1979).
[3] N. Toshima, Phys. Rev. A **42**, 5739 (1990).
[4] K. Tőkési and G. Hock, Nucl. Instrum. Methods Phys. Res. B **154**, 263 (1999).
[5] R. E. Olson and J. Fiol, J. Phys. B **36**, L365 (2003).
[6] N. Bohr, Philos. Mag. **25**, 1 (1913).
[7] E. R. Custidiano, F. J. Perez de la Rosa, and M. M. Jakas, Phys. Rev. A **66**, 052902 (2002).
[8] H. Bethe and R. Jackiw, *Intermediate Quantum Mechanics* (Benjamin, New York, 1968).
[9] E. Fermi and E. Teller, Phys. Rev. **72**, 399 (1947).
[10] O. Firsov, Sov. Phys. JETP **36**, 1076 (1959).
[11] J. Linhard and M. Scharff, Phys. Rev. **124**, 128 (1961).
[12] I. Nagy, Phys. Rev. A **65**, 014901 (2001).
[13] V. U. Nazarov, J. M. Pitarke, C. S. Kim, and Y. Takada, Phys. Rev. B **71**, 121106(R) (2005).
[14] E. Zaremba, I. Nagy, and P. M. Echenique, Phys. Rev. B **71**, 125323 (2005).
[15] G. Schiwietz, Phys. Rev. A **42**, 296 (1990).
[16] R. Cabrera-Trujillo, Y. Öhrn, E. Deumens, and J. R. Sabin, J. Chem. Phys. **116**, 2783 (2002).
[17] E. Deumens, A. Diz, R. Longo, and Y. Öhrn, J. Chem. Phys. **96**, 6820 (1992).
[18] R. Abrines and I. Percival, Proc. Phys. Soc. London **88**, 861 (1966).
[19] J. S. Cohen, Phys. Rev. A **26**, 3008 (1982).
[20] J. A. Phillips, Phys. Rev. **90**, 532 (1953).
[21] H. K. Reynolds, D. N. Dunbar, W. A. Wentzel, and W. Whaling, Phys. Rev. **92**, 742 (1953).
[22] S. Allision and J. Cuevas, Phys. Rev. **127**, 792 (1962).
[23] G. Reitner, N. Niest, E. Pfaff, and G. Clausnitzer, Nucl. Instrum. Methods Phys. Res. B **44**, 399 (1990).

[24] R. Golser and D. Semrad, Nucl. Instrum. Methods Phys. Res. B **44**, 399 (1992).
[25] M. Agnello *et al.*, Phys. Rev. Lett. **74**, 371 (1995).
[26] G. Schiwietz and P. Grande, Radiat. Eff. Defects Solids **130-131**, 137 (1992).
[27] W. Barkas, J. Dyer, and H. Heckman, Phys. Rev. Lett. **11**, 26 (1963); **11**, 26 (1963).
[28] R. L. Becker and A. D. MacKellar, J. Phys. B **17**, 3923 (1984).